

## Original Paper

# Characterization of Hole Transport Layer in Perovskite Solar Cell via Its Performance and Electronic Structure

Yuka YAMANO\*, Tadaaki TANI\*\*, Takayuki UCHIDA\*

**Abstract:** A hole transport layer (HTL) composed of spiro-OMeTAD as a hole transport material (HTM) in a perovskite solar cell (PSC) with  $\text{CH}_3\text{NH}_3\text{PbI}_3$  as a light-absorber was characterized by observing the performance of the cell with variation of the condition in HTL and correlating the result with the electronic structure of the layers, through which positive holes are transferred. While the time-dependent increase in the work function of the Au anode, the doping of a spiro-OMeTAD layer with Li-TFSI and tBP, and the light irradiation increased the short-circuit current and the open-circuit voltage, they made the Fermi level of the HTL deeper and closer to the HOMO level of the spiro-OMeTAD layer. Namely, the changes in the performances and the electronic structures are in accord with each other to indicate that the transport of positive holes in the spiro-OMeTAD layer was disturbed by positive hole traps in the layer, and could be improved by the changes in the condition of the layer, which decreased the depth and density of positive hole traps. It is noted that the Fermi level of the HTL with high performance should be much lower than that of the systems in equilibrium with ambient atmosphere, providing a problem to be solved for the stabilization of PSC.

**Key words:** Perovskite solar cell, Hole transport layer, Doping, Electronic structure, Photoelectron yield spectroscopy in air

## 1. Introduction

Solar cells with perovskite materials as light-absorbers<sup>1)</sup> have rapidly become to attract keen interests of many researchers because of their significant performances such as high power conversion efficiency (PCE), low cost, and easy attitude for production<sup>2)–8)</sup>. Perovskite solar cell (PSC) was developed by replacing Ru-complexing dyes in dye-sensitized solar cell (DSC) by perovskite materials such as  $\text{CH}_3\text{N}-\text{H}_3\text{PbI}_3$ <sup>1)</sup>. Since perovskite materials tend to decompose when they are in contact with solvents<sup>9)</sup>, an electrolyte solution used for a hole-transporting layer (HTL) in DSC was then replaced by a solid-state hole-transporting material (HTM) such as 2,2',7,7'-tetrakis-(N,N-di-p-methoxyphenylamine) 9,9'-spirobifluorene (spiro-MeOTAD)<sup>10)–16)</sup> and CuSCN<sup>17)–18)</sup>. While CuSCN acting as a p-type semiconductor is available for HTM by itself, it has been reported that spiro-MeOTAD is electrically resistive and becomes to be available for HTL on doping<sup>14)–16)</sup>. However, studies on the interaction between spiro-MeOTAD and dopants<sup>13)</sup> have not yet provided sufficient knowledge to make clear the mechanism of the doping.

One of the authors (TT) made an overview of PSC<sup>19)</sup> from the viewpoint of dye sensitization of silver halide (AgX) photographic systems with cyanine dyes and AgX grains as sensitizers and substrates<sup>20)</sup>, respectively, since the former has been derived from the latter via photo-catalyst with

$\text{TiO}_2$  as a substrate<sup>21)</sup>, DSC with Ru-complexing dyes and  $\text{TiO}_2$  as sensitizers and substrate, respectively<sup>22)</sup>. While the overlapping of electronic clouds among cyanine dyes in AgX photographic systems and Ru-complexing dyes in DSC is small, the electronic energy levels of the lowest unoccupied molecular orbital (LUMO) and the highest occupied one (HOMO) of a sensitizing dye molecule with respect to the conduction band minimum (CBM) and the valence band maximum (VBM) of a substrate are essentially important for the study of the light-induced electron transfer from the dye molecule to the substrate. On the other hand, perovskite materials in PSCs are substantially inorganic semiconductors from the viewpoint of their electronic structures<sup>5)–19)</sup>, it is necessary to treat a perovskite material by making notice of its Fermi level in addition to its CBM and VBM. However, such treatment has not yet been made well.

In this paper, we have studied the electronic structure and behavior of an HTL in a PSC with  $\text{CH}_3\text{NH}_3\text{PbI}_3$  as a light absorber according to the above-stated consideration in order to enhance our understanding of the mechanisms of the doping of spiro-MeOTAD layers and the transport property of positive holes in HTLs of PSC.

Received 1st May 2019; Accepted 4th October 2019.

\*Graduate School of Engineering, Tokyo Polytech. Univ., 1583 Iiyama, Atsugi, Kanagawa 243-0297, Japan

\*\*Fellow, Soc. Photogr. Imaging Jpn., 2933-2 Yoshidajima, Kaisei-machi, Ashigarakami-gun, Kanagawa 258-0021, Japan

## 2. Materials and Experiments

### 2.1 Preparation of PSC

The structure of the PSCs, which were prepared in this study, was a mesoporous type as shown in Fig. 1. A compact TiO<sub>2</sub> layer and then mesoporous TiO<sub>2</sub> layer were formed on an FTO glass, which are composed of pyramid-shaped particles of transparent conductive metal oxide (TCO) on a glass plate to enhance the scattering of incident light, and are used as a transparent electrode for solar cells (AGC Fabric Type-VU). A compact TiO<sub>2</sub> layer was formed on a hot plate at 400 °C by means of a spray thermal decomposition method with a solution of 0.6 ml of titanium (IV) diisopropoxide bis (acetylacetonate) (Tokyo Chemical Industry Co., Ltd.) in 8 ml of ethanol. A mesoporous TiO<sub>2</sub> layer with mean pore diameter of 18 nm was formed by spin-coating a suspension of 2g of TiO<sub>2</sub> paste containing 17wt% of TiO<sub>2</sub> particles with ~20 nm in size in water (JGC Catalysts & Chemicals Ltd., PST-18NR) in 7g of ethanol with 5000 rpm at 25 °C and annealing it at 500 °C for 20 min. Then, a layer of CH<sub>3</sub>NH<sub>3</sub>PbI<sub>3</sub> was formed on the above-stated layers by the one step method. Namely, a solution of CH<sub>3</sub>NH<sub>3</sub>I (Wako Pure Chemical Corp.) and PbI<sub>2</sub> (Sigma-Aldrich) (mole ratio of 1:1) in DMF dehydrated (Wako Pure Chemical Corp.) (45 wt%) was coated on the above-stated layers by a spin-coater with 2000 rpm for 30 sec and heated on a hot plate at 70 °C for 30 min to volatilize DMF. An HTL layer and an anode were then formed on the above-stated perovskite layer. In this paper, spiro-OMeTAD and Au were used as HTL and anode, respectively. A layer of spiro-OMeTAD (LT-S922, Luminescence Technology Corp.) was formed by spin-coating its chlorobenzene solution (12 wt%) with 3000 rpm for 30s. In this study, Li-TFSI and tBP<sup>23) 24)</sup> were used as dopants for an HTL layer of spiro-MeOTAD. The former was added to a final concentration of 0.064M, while the latter was added to a final concentration of 0.193M. The chemical structures of these compounds are shown in Fig. 1. An anode was pre-

pared by depositing Au in vacuum on the surface of the HTL.

### 2.2 Analyses of HTL in PSC

The performances of the above-stated cells such as current-voltage (I-V) characteristics, open-circuit voltage ( $V_{oc}$ ), short-circuit current ( $J_{sc}$ ), fill factor (FF), and power conversion efficiency (PCE) were evaluated by means of a solar simulator (HAL-320, Asahi Spectra), an apparatus for the measurement of I-V characteristics (Peccell IV Analyzer 2.2 and Keithley 2400) with 1SUN (100 mW/cm<sup>2</sup>) and AM (Air Mass) 1.5G. The light intensity was calibrated by the 1SUN checker, which was attached to HAL-320. The performances of the above-stated cells were traced for 20 days in room air without any barrier film to get the information of their stability.

The work function, i.e., the energy difference between the highest occupied level (Fermi level for Au, VBM for CH<sub>3</sub>NH<sub>3</sub>PbI<sub>3</sub>, and HOMO for spiro-OMeTAD) and the vacuum level were measured by means of photoelectron yield spectroscopy in air (PYSA; Riken Keiki AC-2)<sup>25)</sup> and compared with the performances of the cells in this study. Every PYSA measurement was carried out in room air at room temperature in the range from 3.80 to 6.20 eV with energy step of 0.05 eV by use of a light source (10 nW). Photoelectrons are captured by oxygen molecules in air to form superoxide radicals (O<sub>2</sub><sup>-</sup>). Then, superoxide radicals are collected and dissociated for the measurement of the yield of photoelectrons in an open counter. The distribution of the measured values for a sample with different experimental condition was small. The standard deviation for the measurement of the work function of an Au layer was ±0.02 eV. The work function of a thin layer of Au used as an anode in the cell was traced for 20 days in room air. The electronic structures of CH<sub>3</sub>NH<sub>3</sub>PbI<sub>3</sub>/HTM/Au, through which positive holes were transported in the cell, were studied as follows. The measurement of the work functions of CH<sub>3</sub>NH<sub>3</sub>PbI<sub>3</sub>, HTM, and Au layers on glasses was made by means of PYSA, and followed by the measurement of the work functions of CH<sub>3</sub>NH<sub>3</sub>PbI<sub>3</sub>/HTM and CH<sub>3</sub>NH<sub>3</sub>PbI<sub>3</sub>/HTM/Au. The electronic structures of CH<sub>3</sub>NH<sub>3</sub>PbI<sub>3</sub>/HTM/Au was constructed with respect to the vacuum level on the basis of the results of the above-stated measurements by taking into account the Fermi levels of CH<sub>3</sub>NH<sub>3</sub>PbI<sub>3</sub>, which should be equalized to those of spiro-OMeTAD and Au to transfer positive holes.

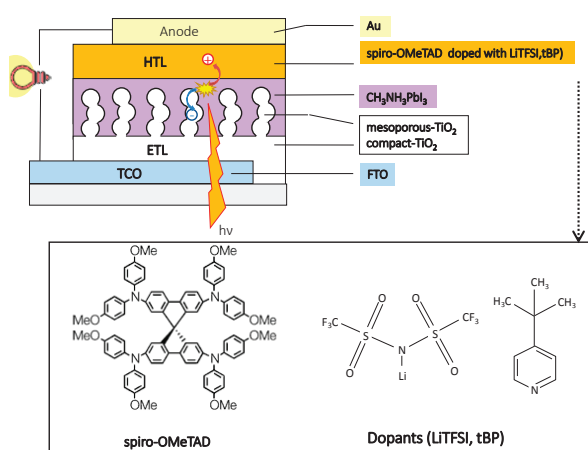


Fig. 1 Cross sectional diagram showing the structure of a perovskite solar cell studied (upper), and chemical structures of spiro-OMeTAD, Li-TFSI, and tBP used for its hole transport layer (lower).

## 3. Results and Discussions

### 3.1 Change in condition of HTL

It is demonstrated in this study that the performance of PSC was markedly influenced by the following three kinds of changes in the positive hole transport in the cells; the time-dependent change in the work function of an Au anode,

the doping of a spiro-OMeTAD layer with Li-TFSI and tBP, and the irradiation of the cells to light.

Fig. 2 shows the time-dependent change in the work function of a thin Au layer in room air, indicating that the work function is increasing with time after its preparation. It is known that the work function of pure Au in vacuum is 5.1 eV<sup>26)</sup>, while that of a thin Au layer in room air becomes to be about 4.8 eV owing to the pinning of its Fermi level to that of an organic layer deposited from air on its surface<sup>27)</sup>. According to a jellium model, the outermost surface region inside a metal is positively charged, and the same amount of the negative charge with electrons is spilled out to several Å in vacuum, forming an electric double layer<sup>26)</sup>. Then, the work function of a metal layer is decreased by the push-back effect, according to which the electric double layers thus formed are depressed by a phenomenon where spilled electrons are pushed back to the inside of the metal when the metal is in contact with an organic layer<sup>26) 27)</sup>. It is considered that the work function of a thin Au layer first decreased owing to the push-back effect when it was in contact with a thin organic layer coming from air, and then increased owing to the pinning of its Fermi level to that of the organic layer coming from air<sup>27)</sup>.

Fig. 3 shows the time-dependent change in the I-V characteristics of the cell, indicating that both  $V_{oc}$  and  $J_{sc}$  increased during its storage for 4 days after its preparation. The increase of  $V_{oc}$  with time was in accord with the in-

crease in the work function of a thin Au layer with time after its preparation (Fig. 2). While the big change in work function taking place for such a short period as seen in Fig. 2 is quite probable and verified for metals including Au in air<sup>27)</sup>, it is not considered to be probable for organic materials available for electronic devices. It is therefore considered that the time-dependent increase in the work function of the Au anode in the cell brought about the time-dependent increase in  $V_{oc}$ . While the work function of a thin Au layer kept for 20 days after its preparation was larger than that of the layer kept for 4 days,  $V_{oc}$  of the cell kept for 20 days in air after its preparation was smaller than that of the cell kept for 4 days. It is considered that this discrepancy arose from the fact that the degradation of a  $\text{CH}_3\text{NH}_3\text{PbI}_3$  layer in the cell was in progress as observed in the previous paper<sup>28)</sup> since the cells were kept in air without any barrier film.

Then, the HTL composed of a thin spiro-OMeTAD layer was doped with Li-TFSI and tBP<sup>23) 24)</sup> according to the procedure described in the previous section. Two cells with undoped and doped spiro-OMeTAD layers as HTLs were prepared and subjected to the measurements of their performances at different 16 positions in each cell. The results are shown in Fig. 4. The averaged values and their coefficients of variation are listed in the tables in Fig. 4. The fluctuation of the performances of the cells with an un-doped spiro-OMeTAD layer was large, especially for  $J_{sc}$ , and could be much improved by the doping.

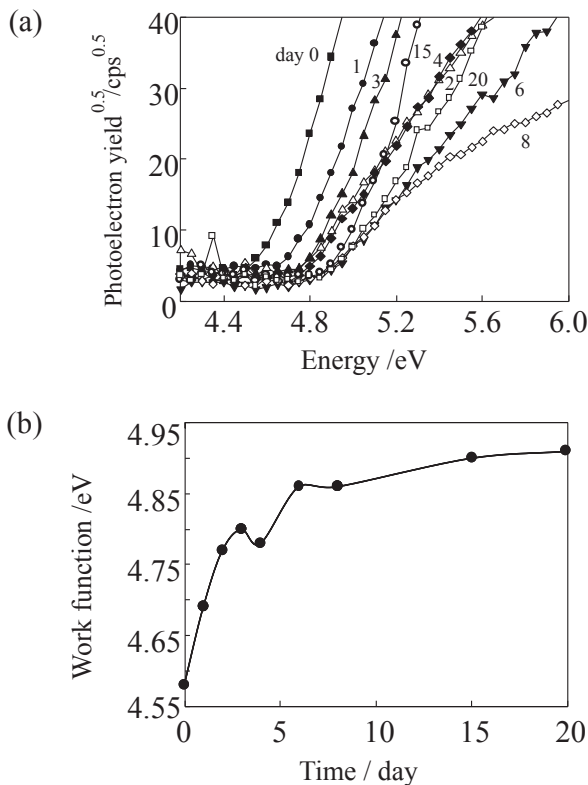


Fig. 2 Time-dependent change in the PYSA spectrum (a) and work function (b) of a thin Au layer, which was prepared in vacuum and then kept in ambient atmosphere for the time period indicated on each spectrum (a) and the abscissa (b).

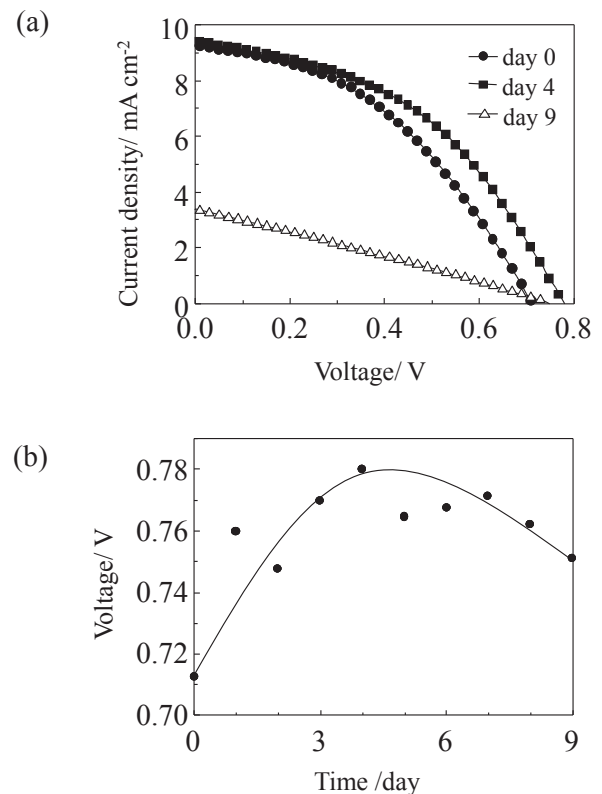


Fig. 3 Time-dependent changes in J-V curve characteristics (a) and open-circuit voltage (b) of a perovskite solar cell composed of FTO/ $\text{TiO}_2$ / $\text{CH}_3\text{NH}_3\text{PbI}_3$ /spiro-OMeTAD/Au.

Fig. 5 shows the PYSA spectra of an un-doped spiro-OMeTAD layer,  $\text{CH}_3\text{NH}_3\text{PbI}_3$ /un-doped spiro-OMeTAD layers, and  $\text{CH}_3\text{NH}_3\text{PbI}_3$ /doped spiro-OMeTAD layers. While the work function of spiro-OMeTAD was hardly influenced by its contact with MAPbI<sub>3</sub>, it was significantly increased by the doping. It is considered from this result that the dopants drew electrons from the spiro-OMeTAD layer to bring about the increase in its work function and to decrease the photoelectron yields from it. Fig. 6 shows the PYSA spectra of un-doped spiro-OMeTAD/Au layers,  $\text{CH}_3\text{NH}_3\text{PbI}_3$ /un-doped spiro-OMeTAD/Au layers, and  $\text{CH}_3\text{NH}_3\text{PbI}_3$ /doped spiro-OMeTAD/Au layers. The doping significantly decreased the photoelectron yield from Au layer in this system, and increased the work function of the Au layer. It is considered from this result that the dopants drew electrons from the spiro-OMeTAD layer to lower its Fermi level and that of the Au anode, decreasing the photoelectron yield from the Au anode.

Fig. 7 shows the effect of irradiation on the PYSA spectra of the PSCs with undoped spiro-OMeTAD layer as an HTL. As seen in this figure, the irradiation increased the work function of the Au anode of the cell and decreased the photoelectron field from it. It is considered from the result in this figure that positive holes created in the  $\text{CH}_3\text{NH}_3\text{PbI}_3$  layer in the cell were transferred to the spiro-OMeTAD

layer and captured by traps to deepen the Fermi levels of the spiro-OMeTAD layer and the Au anode of the cell, and that the above-stated condition created by the light irradiation was kept for a relatively long time (more than 5 min).

**3.2 Electronic structures of HTL**

Fig. 8 (a) and (b) show the electronic structures of  $\text{CH}_3\text{NH}_3\text{PbI}_3$ /undoped spiro-OMeTAD/Au and  $\text{CH}_3\text{NH}_3\text{PbI}_3$ /

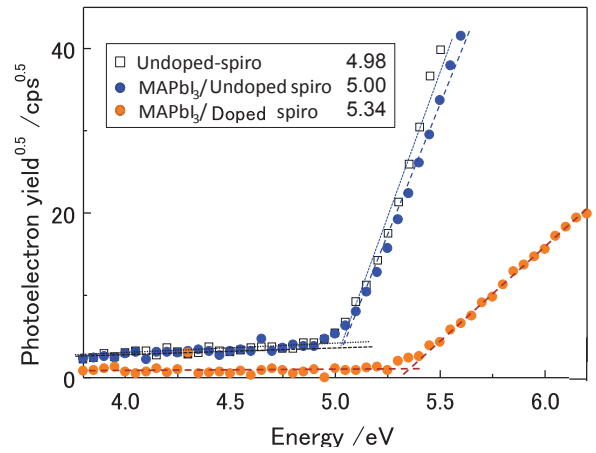


Fig. 5 PYSA spectra of an undoped spiro-OMeTAD layer,  $\text{CH}_3\text{NH}_3\text{PbI}_3$ /undoped spiro-OMeTAD layers, and  $\text{CH}_3\text{NH}_3\text{PbI}_3$ /doped spiro-OMeTAD layers. An inserted table shows their work functions.

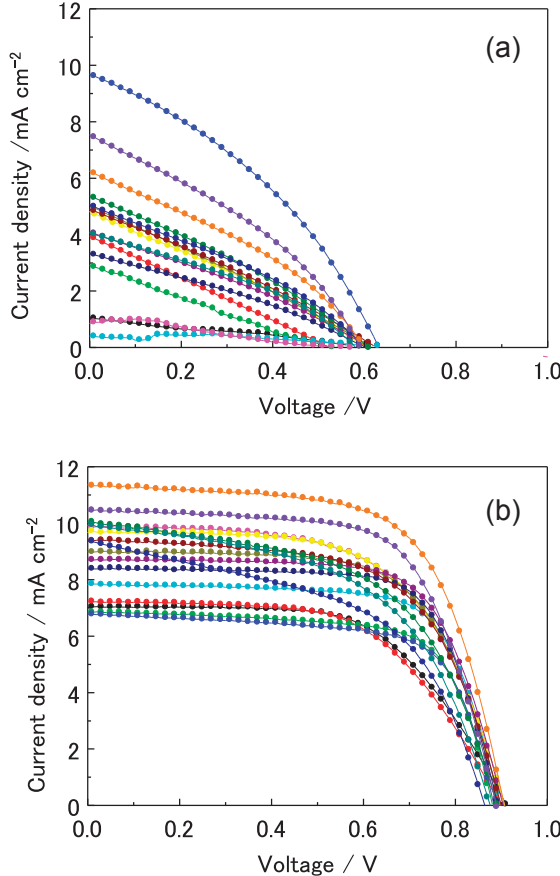


Fig. 4 I-V characteristics of perovskite solar cells with undoped (a) and doped (b) spiro-OMeTAD/Au layers as measured at 16 different points on each cell. Upper and lower tables show the average values and coefficients of variation (CV) of the performances of the cells with I-V characteristics shown in (a) and (b), respectively.

	Average	Coefficient variation
$J_{sc} / \text{mA cm}^{-2}$	4.33	0.54
$V_{oc} / \text{V}$	0.6	0.06
F.F.	0.31	0.15
PCE / %	0.82	0.64



Doping of spiro (HTM)

	Average	Coefficient variation
$J_{sc} / \text{mA cm}^{-2}$	8.87	0.15
$V_{oc} / \text{V}$	0.89	0.01
F.F.	0.83	0.1
PCE / %	4.96	0.15

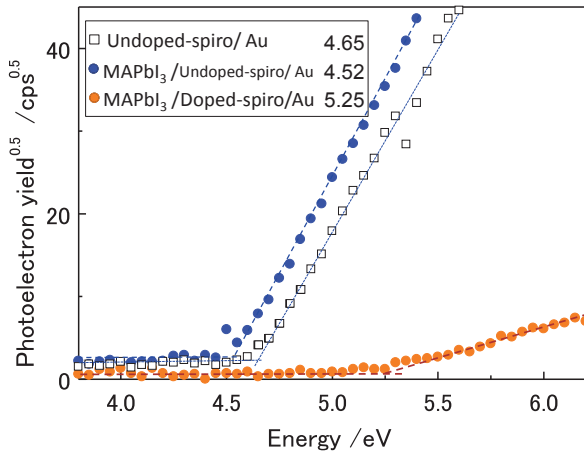


Fig. 6 PYSA spectra of undoped spiro-OMeTAD/Au layers,  $\text{CH}_3\text{NH}_3\text{PbI}_3$ /undoped spiro-OMeTAD/Au layers, and  $\text{CH}_3\text{NH}_3\text{PbI}_3$ /doped spiro-OMeTAD/Au layers. An inserted table shows their work functions.

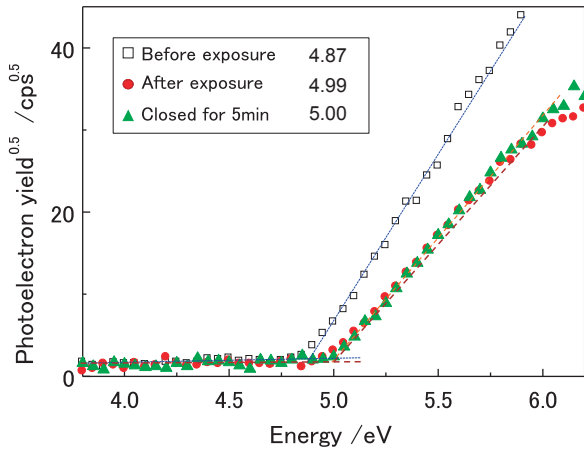


Fig. 7 PYSA spectra of a perovskite solar cell composed of FTO/TiO<sub>2</sub>/CH<sub>3</sub>NH<sub>3</sub>PbI<sub>3</sub>/spiro-OMeTAD/Au before and after exposure to light, and after 5 min since the exposure was ceased.

doped spiro-OMeTAD/Au layers, respectively, as constructed with respect to the vacuum level according to the process described in Section 2.2. In Fig. 8 (a), the ionization energies of  $\text{CH}_3\text{NH}_3\text{PbI}_3$  and spiro-OMeTAD were measured in this study as 5.52 eV and 4.98 eV, respectively. The ionization energy of Au was reported as 5.1 eV<sup>26</sup>. The ionization energy of spiro-OMeTAD on  $\text{CH}_3\text{NH}_3\text{PbI}_3$  was measured as 5.00 eV, indicating the vacuum level shift as -0.02 eV. The ionization energy (i.e., work function) of Au on spiro-OMeTAD/ $\text{CH}_3\text{NH}_3\text{PbI}_3$  was measured as 4.52 eV, indicating that the vacuum level shift between spiro-OMeTAD and Au was 0.60 eV, and that the Fermi level of spiro-OMeTAD was by 0.48 eV higher than its HOMO level. The electronic structure in Fig.8 (b) was constructed similarly.

While the orientation of the single crystals of metals and organic semiconductors influence their work functions<sup>30</sup>, they are not taken into account for the construction of the electronic structures in Fig. 8, since the samples were amorphous or polycrystalline with randomly oriented small crystallites. As seen in Fig. 8 (a), the Fermi level of the Au anode

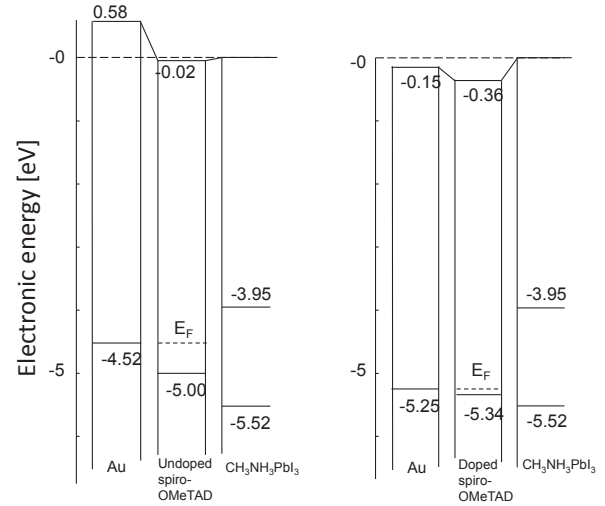


Fig. 8 Electronic structures of (a)  $\text{CH}_3\text{NH}_3\text{PbI}_3$ /undoped spiro-OMeTAD/Au layers and (b)  $\text{CH}_3\text{NH}_3\text{PbI}_3$ /doped spiro-OMeTAD/Au layers, where  $E_f$  indicates the position of Fermi level in a spiro-OMeTAD layer.

in the layer with an undoped spiro-OMeTAD, which was measured immediately after the preparation of the film, was -4.52 eV, being higher by 0.48 eV than the HOMO level of a spiro-OMeTAD in the layer. This result indicates that positive hole traps with  $\leq 0.48$  eV in depth were present and should hinder the transport of positive holes in an undoped spiro-OMeTAD layer by trapping them. The Fermi level of the Au anode was close to that of Au layer immediately after its preparation, which then increased by  $\sim 0.3$  eV on its storage in air for 4 days as seen in Fig. 2.

The comparison between Fig. 8 (a) and (b) reveals that the dopants could lower the Fermi levels of, not only spiro-OMeTAD layer, but also Au anode and  $\text{CH}_3\text{NH}_3\text{PbI}_3$  layer by drawing electrons from the spiro-OMeTAD layer. In the undoped spiro-OMeTAD layer, positive hole traps with  $\leq 0.48$  eV in depth were present and captured positive holes. On the other hand, only traps with  $\leq 0.09$  eV in depth were present and captured positive holes in the doped spiro-OMeTAD layer. This result could provide an explanation for the observed result that the values of  $J_{sc}$  of the cell could be significantly improved and their coefficient of variation could be much decreased by the doping. In addition, it is considered that the big increase in the work function of the Au anode by the dopants contributed to the increase of  $V_{oc}$  of the cell by the dopants.

As discussed above, the electronic structure of a spiro-OMeTAD layer in a device could be evaluated and has turned out to be useful for studying the behavior of positive holes in the layer responsible for the performance of the device. The usefulness of the knowledge of the electronic structure should be further enhanced when it would be supported by the measurements of the conductivity, mobility of positive holes, number and depth of positive hole traps in a spiro-OMeTAD layer.

#### 4. General Discussions

In order to characterize the performance of a PSC from the viewpoint of its electronic structure, the performance of a PSC composed of FTO/TiO<sub>2</sub>/CH<sub>3</sub>NH<sub>3</sub>PbI<sub>3</sub>/spiro-OMeTAD/Au was studied with variation of factors relating to the layers, through which positive holes were transferred. Then, the results were correlated with the electronic structure of CH<sub>3</sub>NH<sub>3</sub>PbI<sub>3</sub>/spiro-OMeTAD/Au layers, which were constructed from the PYSA spectra of individual and combined layers of their components, as shown in Fig. 8.

The electronic structures of the CH<sub>3</sub>NH<sub>3</sub>PbI<sub>3</sub>/spiro-OMeTAD/Au layers were constructed under the assumptions that the Fermi levels were present in individual layers of its components and brought about the electron transfer phenomena to equalize the Fermi levels among them. Since the electronic structure of CH<sub>3</sub>NH<sub>3</sub>PbI<sub>3</sub> is substantially an inorganic semiconductor, its Fermi level was measured and discussed in many papers<sup>19) 29)</sup>. Although spiro-OMeTAD is an organic semiconductor, the Fermi level of a spiro-OMeTAD layer and its role in the electronic phenomena in the layer were discussed in the literature<sup>13) 15)</sup>. It is therefore considered that the equalization of Fermi level took place at the interface between the spiro-OMeTAD/CH<sub>3</sub>NH<sub>3</sub>PbI<sub>3</sub> layers as well as the interface between the spiro-OMeTAD/Au layers.

The Fermi level equalization should bring about the shift of the vacuum levels of the layers involved<sup>26) 30)</sup>. The shift takes place at the interface between them without band-bending in the layers when the transferred electrons are mostly located at the interface. On the other hand, the shift takes place between the bulks with band-bending in the layers involved when the transferred electrons located, not at their interface, but in the bulks of the layers involved.

Kahn and others did not observe any band-bending in a CH<sub>3</sub>NH<sub>3</sub>PbI<sub>3</sub> layer when the Fermi level equalization took place on its contact with a TiO<sub>2</sub> layer<sup>29)</sup>. It is therefore considered that the Fermi level equalization between CH<sub>3</sub>NH<sub>3</sub>PbI<sub>3</sub> and spiro-OMeTAD did not bring about any band-bending in the former. Seki and Ishii observed the vacuum level shift at the interface between many organic semiconductors and substrates when they were in contact with each other<sup>26)</sup>. In this paper, it is therefore considered that the Fermi level equalization of a spiro-OMeTAD layer with a CH<sub>3</sub>NH<sub>3</sub>PbI<sub>3</sub> layer and an Au layer took place to cause the vacuum level shifts at the interfaces, as shown in Fig. 8. Fig. 8 shows the vacuum level shifts at the interfaces between spiro-OMeTAD and CH<sub>3</sub>NH<sub>3</sub>PbI<sub>3</sub> layers and those between spiro-OMeTAD and Au layers without and with Li-TFSI, which have been observed for the first time to our best knowledge, and reflected the electron transfer across the interfaces. The observed vacuum level shift at the interface between undoped spiro-OMeTAD and CH<sub>3</sub>NH<sub>3</sub>PbI<sub>3</sub> was not however large enough to indicate the presence of any substantial

electron transfer between them.

The short-circuit current of the PSCs prepared in this study was increased by the doping of a spiro-OMeTAD layer with Li-TFSI and tBP. Being in accord with the electronic structures of the systems studied in this paper, the change in the condition of HTL by the doping is considered to make the Fermi level of the spiro-OMeTAD layer closer to its HOMO level, and therefore to make the positive hole traps shallower. This result indicates that positive hole traps in a spiro-OMeTAD layer disturb the transport of positive holes in it, and could be almost eliminated by the dopants employed in this study.

These results are in good accord with the observation that the traps in a spiro-OMeTAD are filled by such a p-type dopant as Li-TFSI and light-created positive holes to exhibit ESR spectra attributable to long-lived positive holes in it<sup>31)</sup>. It is therefore considered that positive hole traps in spiro-OMeTAD layers are situated at the HOMO levels of their molecules with wide distribution owing to their disordered condition.

As seen in Fig. 7, the change caused in a PSC by irradiation was kept for a relatively long time. A PSC usually exhibits severe hysteresis in I-V measurement and is being studied in relation to some slow processes responsible for it<sup>32) 33)</sup>. However, it seems that such slow processes are derived, not from the accumulation of positive hole traps in HTL as analyzed in this study, but from ion migration or re-orientation of dipoles of methyl ammonium cations in the bulk of CH<sub>3</sub>NH<sub>3</sub>PbI<sub>3</sub>, resulting in the appearance of hysteresis and slow recovery of light-induced changes as seen in Fig. 7.

The Fermi level of thin metal layers including an Au layer however tends to be pinned to the Fermi level of an organic layer deposited from air (estimated to be about 4.8 eV in the previous paper<sup>27)</sup>), as observed in Fig. 2. The work function of the Au anode on the doped spiro-OMeTAD layer was 5.25 eV and larger than that of an organic layers deposited from air. It is probable that the Fermi level of the Au anode in the cells tends to be pinned to that of an organic layer deposited from air when the cell will be kept in air. This phenomenon should bring about the electron transfer from the organic layer to the Au anode, and then the electron transfer from the Au anode to the doped spiro-OMeTAD layer. It is concerned that this change with time deteriorate the positive hole transport in the doped spiro-OMeTAD layer by increasing the depth and density of positive hole traps in it, indicating the necessity to keep the cell apart from air for the stabilization of its performance.

#### References

- 1) Akihiro Kojima, Kenjiro Teshima, Yasuo Shirai, and Tsutomu

- Miyasaka, "Organometal Halide Perovskites as Visible-Light Sensitizers for Photovoltaic Cells", *J. Am. Chem. Soc.*, **131**, 6050-6051 (2009).
- 2) Henry J. Snaith, "Perovskites: The Emergence of a New Era for low-Cost, High-efficiency Solar Cells", *J. Phys. Chem. Lett.*, **4**, 3623-3630 (2013).
  - 3) Hyun Suk Jung, Nam-Gyu Park, "Perovskite Solar Cells: From Materials to Devices", *Small*, **11**, 10-25 (2015).
  - 4) Tsutomu Miyasaka, "Perovskite Photovoltaics: Rare Functions of Organo Lead Halide in Solar Cells and Optoelectronic Devices", *Chem. Lett.*, **44**, 720-729 (2015).
  - 5) Yoshihiko Kanemitsu, Yasuhiro Yamada, Takumi Yamada, "Free Carrier Radiative Recombination and Photon Recycling in Lead Halide Perovskite Solar Cell Materials", *Bull. Chem. Soc. Jpn.*, **90**, 1129-1140 (2017).
  - 6) Tsutomu Miyasaka, "Lead Halide Perovskites in Thin Film Photovoltaics: Background and Perspective", *Bull. Chem. Soc. Jpn.*, **91**, 1058-1068 (2018).
  - 7) Jotaro Nakazaki, Hiroshi Segawa, "Evolution of organometal halide solar cells", *J. Photochem. Photobiol. C: Photochemistry Reviews*, **35**, 74-107 (2018).
  - 8) Ajai Kumar Jena, Ashish Kulkarni, Tsutomu Miyasaka, "Halide Perovskite Photovoltaics: Background, Status, and Future Prospect", *Chem. Rev.*, **119**, 3036-3103 (2019).
  - 9) Jinli Yang, Braden D. Siempelkamp, Dianyi Liu, Timothy L. Kelly, "Investigation of  $\text{CH}_3\text{NH}_3\text{PbI}_3$  Degradation Rates and Mechanisms in Controlled Humidity Environments Using in Situ Techniques", *ACS nano*, **9**, 1955-1963 (2015).
  - 10) U. Bach, D. Lupo, P. Comte, J. E. Moser, F. Weissoertel, J. Salbeck, H. Spreitzer, & M. Graetzel, "Solid-state dye-sensitized mesoporous  $\text{TiO}_2$  solar cells with high photon-to-electron conversion efficiencies", *Nature*, **395**, 583-585 (1998).
  - 11) Hui-Seon Kim, Chang-Ryul Lee, Jeong-Hyeok Im, Ki-Beon Lee, Thomas Moehl, Arianna Marchioro, Soo-Jin Moon, Robin Humphry-Baker, Jun-Ho Yum, Jacques E. Moser, Michael Grätzel, Nam-Gyu Park, "Lead Iodide Perovskite Sensitized All-Solid-State Submicron Thin Film Mesoscopic Solar Cell with Efficiency Exceeding 9%", *Scientific Reports*, **2**, 591 (2012).
  - 12) Michael M. Lee, Joël Teuscher, Tsutomu Miyasaka, Takurou N. Murakami, Henry J. Snaith, "Efficient Hybrid Solar Cells Based on Meso-Superstructured Organometal Halide Perovskites", *Science*, **338**, 643-647 (2012).
  - 13) Rebecka Schoelin, Martin H. Karlson, Susanna K. Erikson, Hans Siegbahn, Erik M. J. Johansson, "Energy Level Shifts in Spiro-OMeTAD Molecular Thin Films When Adding Li-TFSI", *J. Phys. Chem. C* **116**, 26300-26305 (2012).
  - 14) Ute B. Cappel, Torben Daeneke, Udo Bach, "Oxygen-Induced Doping of Spiro-MeOTAD in Solid-State Dye-Sensitized Solar Cells and Its Impact on Device Performance", *Nano Letters*, **12**, 4925-4931 (2012).
  - 15) Mi Xu, Yaoguang Rong, Zhiliang Ku, Anyi Mei, Xiong Li, Hongwei Han, "Improvement in Solid-State Dye Sensitized Solar Cells by p-Type Doping with Lewis Acid  $\text{SnCl}_4$ ", *J. Phys. Chem. C* **117**, 22492-22496 (2013).
  - 16) Antonio Abate, Daniel R. Staff, Derek J. Hollman, Henry J. Snaith, Alison B. Walker, "Influence of ionizing dopants on charge transport in organic semiconductors", *Phys. Chem. Chem. Phys.*, **16**, 1132-1138 (2014).
  - 17) Peng Qin, Soichiro Tanaka, Seigo Ito, Nicolas Tetreault, Kyohei Manabe, Hitoshi Nishino, Mohammad Khaja Nazeerudien, Michael Graetzel, "Inorganic hole conductor-based lead halide perovskite solar cells with 12.4% conversion efficiency", *Nature Commun.*, **2014**, DOI:10.1038/ncomms4834.
  - 18) Seigo Ito, Soichiro Tanaka, Henri Vahlman, Hitoshi Nishino, kyohei Manabe, Peter Lund, "Carbon-Double-Bond-free Printed Solar Cells from  $\text{TiO}_2/\text{CH}_3\text{NH}_3\text{PbI}_3/\text{CuSCN}/\text{Au}$ : Structural control and Photoaging Effects", *ChemPhysChem* **15**, 1194-1200 (2014).
  - 19) Tadaaki Tani, "Survey of Perovskite Solar Cells from Dye Sensitization in Silver Halide Photographic Systems", *J. Soc. Photogr. Imaging Jpn.*, **81**, 318-333 (2018).
  - 20) Tadaaki Tani, "Photographic Science Advances in Nanoparticles, J-Aggregates, Dye Sensitization, and Organic Devices", Oxford University Press, Oxford, 2011.
  - 21) Akira Fujishima and Kenichi Honda, "Electrochemical Photolysis of Water at a Semiconductor Electrode", *Nature*, **238**, 37-38 (1972).
  - 22) Brian O'Regan and Michael Graetzel, "A low-cost, high-efficiency solar cell based on dye-sensitized colloidal  $\text{TiO}_2$  films", *Nature*, **353**, 737-740 (1991).
  - 23) Shen Wang, Mahsa Sina, Pritesh Parikh, Taylor Uekert, Brian Shabazian, Arun Devaraj, Ying Shirley Meng, "Role of 4-tert-Butylpyridine as a Hole Transport Layer Morphological Controller in Perovskite Solar Cells", *Nano Lett.*, **16**, 5594-5600 (2016).
  - 24) Naoki Ishida, Atsushi Wahamiya, Akinori Saeki, "Quantifying Hole Transfer Yield from Perovskite to Polymer Layer: Statistical Correlation of Solar Cell Outputs with Kinetic and Energetic Properties", *ACS Photonics*, **3**, 1678-1688 (2016).
  - 25) Y. Nakajima, M. Hoshino, D. Yamashita, and M. Uda, "Near Edge Structure of Mg-, Co-, Cu-, and Zn-Tetraphenylporphyrins Measured by PESA and Calculated with DV-X  $\alpha$ ", *Advances in Quantum Chemistry*, **42**, 399-405 (2003).
  - 26) Hisao Ishii and Kazuhiko Seki, "Energy Level Alignment at Organic-Metal Interfaces", in "Conjugated Polymer and Molecular Interfaces Science and Technology for Photonic and Optoelectronic Applications", William R. Salaneck, Kazuhiko Seki, Antoine Kahn, and Jean-Jacques Pireaux, eds., Marcel Dekker, Inc., New York, Basel, 2001, pp.293-349.
  - 27) Tadaaki Tani, Ryota Kan, Yuka Yamano, Takayuki Uchida, "Stabilization of Ag nanostructures by tuning their Fermi levels", *Jpn. J. Appl. Phys.*, **57**, 055001 (2018).
  - 28) Yuka Yamano, Ryota Kan, Tadaaki Tani, Takayuki Uchida, "Characteristics of the Hole Transport in Perovskite Solar Cells and Their Aging Effects", *J. Soc. Photogr. Imaging Jpn.*, **80**, 53-59 (2017).
  - 29) Phillip Schulz, Eran Edri, Saar Kirmayer, Gary Hodes, David Cahen, Antoine Kahn, "Interface energetics in organo-metal halide perovskite-based photovoltaic cells", *Energy & Environ. Sci.*, **7**, 1377-1381 (2014).
  - 30) Tadaaki Tani (supervised by Hiroo Inokuchi), "Fundamentals and Principles of Organic Semiconductors in Light of Inorganic Semiconductors and Silver Halide Photography", Maruzen Pub. Co., Tokyo, 2014.
  - 31) Miki Namatame, Masaki Yabusaki, Takehiro Watanabe, Yuhei Ogomi, Shuzi Hayase, Kazuhiro Marumoto, "Direct observation of dramatically enhanced hole formation in a perovskite-solar-cell material spiro-OMeTAD by Li-TFSI doping", *Appl. Phys. Lett.*, **110**, 123904 (2017).
  - 32) Henry J. Snaith, Antonio Abate, James M. Ball, Giles E. Eperon, Thomas Leijtens, Nakita K. Noel, Samuel D. Stranks, Jacob Tse-Wei Wang, Konrad Wojciechowski, Wei Zhang, "Anomalous Hysteresis in Perovskite Solar Cells", *J. Phys. Chem. Lett.*, **5**, 1511-1515 (2014).
  - 33) E. L. Unger, E. T. Hoke, C. D. Bailie, W. H. Nguyen, A. R. Bowring, T. Heumüller, M. G. Christoforo, M. D. McGehee, "Hysteresis and transient behavior in current-voltage measurements of hybrid-perovskite absorber solar cells", *Energy & Environmental Science*, **7** (11), 3690-3696 (2014).